Journal of
MASS SPECTROMETRY

Received: 14 December 2010 Accepted: 10 September 2010

(wileyonlinelibrary.com) DOI 10.1002/jms.1847

Energy-dependent dissociation of benzylpyridinium ions in an ion-trap mass spectrometer

Emilie-Laure Zins,[a,b] Claude Pepe[b] and Detlef Schröder[a]*

Benzylpyridinium ions, generated via electrospray ionization of dilute solutions of their salts in acetonitrile/water, are probed by collisional activation in an ion-trap mass spectrometer. From the breakdown diagrams obtained, phenomenological appearance energies of the fragment ions are derived. Comparison of the appearance energies with calculated reaction endothermicities shows a reasonably good correlation for this particular class of compounds. In addition, the data indirectly indicate that at threshold the dissociation of almost all of the benzylpyridinium ions under study leads to the corresponding benzylium ions, rather than the tropylium isomers. Substituent effects on the fragmentation for a series of benzylpyridinium ions demonstrate that neither mass effects nor differences in density of states seriously affect the energetics derived from the ion-trap experiments. Copyright © 2010 John Wiley & Sons, Ltd.

Keywords: benzylpyridinium ions; collision-induced dissociation; electrospray ionization; mass spectrometry

Introduction

In addition to numerous applications in analytical sciences, mass spectrometry is known as a powerful tool for the determination of intrinsic thermodynamic properties of gaseous ions. The kinetic method,[1] for example, provides a rapid and easy way for the accurate determination of relative properties such as gas-phase acidities and basicities, including the differentiation of stereoisomers.[2] Similarly, collision-induced dissociation (CID) experiments can provide accurate bond dissociation and/or activation energies, depending on whether thermodynamic or kinetic control is operative.[3,4] Unlike the relative binding energies in the kinetic methods, the conversion of the raw threshold data into absolute bond energies often is not trivial, however, because several effects, including instrumental parameters, may play a role, and the conversion of the activation parameters into an energy scale is not always straightforward.[5] Even more complex is the situation in ion-trap mass spectrometers (IT-MS)[6,7] in which collisional activation of the stored ions is affected by RF-excitation of the ions, which leads to multiple collisions of the ions with the helium buffer gas present in the trap. Hence, CID experiments are easy to perform in IT-MS, but their quantitative analysis is difficult. For instance, in the case of the Thermo Finnigan LCQ IT-MS, only normalized collision energies (NCEs) can be obtained experimentally. These values, given as percentages of a 'standard' activation pulse, depend on the mass of the parent ion with the aim to achieve a similar amount of excitation for ions of different masses.[8] It would thus be beneficial if a method to convert these experimental values into activation energies were available.

Here, we seek for correlations between the phenomenological appearance energies (AEs) determined in the NCE framework of an IT-MS and the activation energies for a family of compounds.[9] For this purpose, we have chosen the loss of pyridine from substituted benzylpyridinium ions [R-C_6H_4-CH_2-NC_5H_5]$^+$ (Scheme 1) which are frequently used as 'thermometer ions' to evaluate internal energy distributions.[10–29]

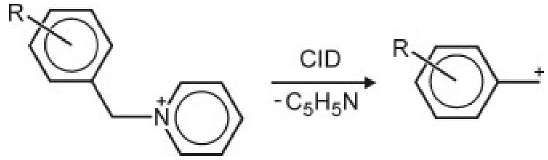

Scheme 1. Generation of benzylium ions upon CID of benzylpyridinium ions concomitant with the loss of neutral pyridine.

In a series of previous experimental and theoretical studies, we have revisited the loss of pyridine from substituted benzylpyridinium ions. Depending on the substituents, this process occurs either as a direct bond-cleavage reaction or is associated with partial rearrangement of the product ions into the corresponding tropylium isomers.[30–32] Here, we apply the theoretically predicted activation energies of these fragmentation reactions in order to probe possible correlations with the phenomenological AEs obtained in IT-MS. In this context, a reviewer noted that Hoxha *et al.*[33] have previously studied the energy deposition in ions under multiple collision conditions and found a linear relationship between the voltage settings in the ion source and the effective temperature of the ions.

---

* Correspondence to: Detlef Schröder, Institute of Organic Chemistry and Biochemistry, Flemingovo nám. 2, 16610 Prague 6, Czech Republic. E-mail: detlef.schroeder@uochb.cas.cz

a Institute of Organic Chemistry and Biochemistry, Flemingovo nám. 2, 16610 Prague 6, Czech Republic

b Laboratoire de Dynamique, Interactions et Réactivité, UMR 7075 CNRS/UPMC, Université Pierre et Marie Curie, 4 Place Jussieu, 75252 Paris Cedex 05, France

Experimental and Theoretical Details

The experiments were performed with a Finnigan LCQ IT-MS[34] and a closely similar Finnigan LCQ Deca XP Plus instrument.[30] In brief, the LCQ bears a conventional ESI source consisting of the spray unit (flow rate set to 5 µl min^{-1} and a spray voltage of *ca* 5 kV) with nitrogen as a sheath gas, followed by a heated transfer capillary (kept at 75 °C), a first set of lenses which determine the softness or hardness of ionization by varying the degree of collisional activation in the medium-pressure regime,[35,36] two transfer octopoles, and a Paul ion-trap for ion storage and manipulation in the presence of *ca* 10^{-3} mbar helium as a trapping gas. For detection, the ions are ejected from the trap to an electron multiplier. Mass spectra were recorded from *m/z* 80 to 2000. Low-energy CID was performed by application of an excitation AC voltage to the end caps of the trap to induce collisions of the isolated ions with the helium buffer gas for a period of 20 ms, a trapping parameter $q_z = 0.25$ and variable excitation amplitudes. Furthermore, within the Finnigan software, the isolation width in ion selection also affects the excitation in CID; we have chosen an isolation width to completely separate the ions of interest from their ^{13}C isotopes (in the LCQ, an isolation width of 2 amu is sufficient for this purpose). The collision energy was modified for each experiment and is expressed in terms of the manufacturer's NCE (given in %). The range from 0% to 100% corresponds to a resonance excitation AC signal of 0–2.5 V (zero-to-peak) at the secular frequency of the interest ion. From the side of the software of the instrument, the amplitude applied in NCE depends on the *m/z* value of the parent ion, but this value is not expressed directly in voltage units. In the NCE technology,[8] the peak-to-peak voltage is scaled as $V_{\text{pp}} = \text{NCE}/30 \times (a(m/z) + b)$, where a and b are variable parameters (0.0015 and 0.56, respectively). However, instead of an explicit conversion of the peak-to-peak voltage applied into the effective kinetic energy of the ions in the trap upon RF-excitation, we prefer the pragmatic approach to calibrate the energy scale using independent thermochemical data. The result of energy-dependent CID experiments with a given mass-selected parent ion is a breakdown curve with approximate sigmoid shape (see below). For the quantitative analysis of the breakdown curve, we apply a simple procedure previously derived for CID experiments in multipole mass spectrometers,[37] which has been applied for the determination of AEs of a variety of gaseous transition-metal ions.[38–40] Specifically, following a proposal of Bouchoux *et al*.[41] derived for a different purpose, the energy-dependent CID spectra were modeled by sigmoid functions of the type $I_i(E) = a_i/(1 + e^{(E_{1/2,i} - E)b_i})$ using a least-squares criterion; for the parent ion M, the relation is: $I_{\text{M}}(E) = [1 - (a_i/(1 + e^{(E_{1/2,i} - E)b_i}))]$. Here, a_i stands for the branching ratio of a particular product ion ($\Sigma a_i = 1$), $E_{1/2}$ is the energy at which the sigmoid function has reached half of its maximum, E is the collision energy and b (in eV^{-1}) describes the rise of the sigmoid curve and thus the phenomenological energy dependence; in consecutive dissociations, all higher order product ions are added to the intensity of the primary fragment. The phenomenological AEs are then derived from a numerical linear extrapolation of the rise of the sigmoid curve at $E_{1/2}$ to the baseline. Note that the uncertainty of the extrapolation based on the fitted function is much smaller than the experimental error of repeated measurements.

The details of the theoretical computations were described elsewhere.[30] Briefly, density functional theory (DFT) calculations using B3P86/6-31+G* were performed with the Gaussian 03 software[42] including complete geometry optimization and frequency calculations. The energies reported below include zero point energy (ZPE) correction and refer to 0 K.

The substituted benzylpyridinium salts were prepared by treating the corresponding benzyl halides with excess anhydrous pyridine at 60 °C for 3 h. After the reaction, the excess of pyridine was evaporated to give a solid. The compounds were analyzed by mass spectrometry and used without further purification.[30] All reagents for synthesis were purchased from Sigma–Aldrich (Saint Quentin Fallavier, France).

Results and Discussion

In this work, the well-studied fragmentation of benzylpyridinium ions to the corresponding carbenium ions concomitant with the loss of pyridine (Scheme 1) is used to probe the suitability of ion-trap mass spectrometry for energy-resolved collision experiments for this representative class of compounds. As an example, Fig. 1 shows the breakdown curves obtained in the case of the fragmentation of the *para*-fluoro-benzylpyridinium ion $[p\text{-F-C}_6\text{H}_4\text{-CH}_2\text{-NC}_5\text{H}_5]^+$. At a nominal collision energy of NCE = 17%, the loss of pyridine starts to be observed, then gradually increases at higher collision energies and reaches a plateau when fragmentation of the parent ion is complete. As demonstrated by comparison of the experimental values (symbols) and the modeled data (lines) in Fig. 1, the resulting breakdown graphs can be approximated using sigmoid functions (see Section on Experimental and Theoretical Details), which is purely a phenomenological approach adopted from the analysis of photoionization spectra.[43,44] However, an approximately sigmoid behavior can be deduced by assuming a fully thermal behavior of the ions in the trap upon excitation using the combination of Arrhenius law with a time-constrained ion dissociation: $I_{\text{F}}/I_\Sigma = 1 - I_{\text{P}}/I_\Sigma = 1 - \exp(-A_0 \exp(-E_{\text{a}}/RT_{\text{eff}}) \times t_{\text{diss}})$. Here, I_{F} and I_{P} are relative intensities of the fragment and the parent ion with I_Σ as their sum, A_0 is the pre-exponential factor, E_{a} is the activation energy, R is the gas constant, T_{eff} is an effective temperature describing ion dissociation without a direct physicochemical meaning and t_{diss} is the time window for dissociation (here 20 ms). Using $A_0 = 10^7\ \text{s}^{-1}$ and $E_{\text{a}} = 200\ \text{kJ mol}^{-1}$ as arbitrary input parameters of this simple conceptual model, the resulting profile for the parent and the daughter ions has approximate sigmoid shape and the corresponding derivative is not a perfect Gaussian, but close to it within the energy resolution of the experiments (insets in Fig. 1). While this type of function can also be used to fit the experimental data, the sigmoid fit is preferred on pragmatic grounds, because both approaches fit the experimental data with similar quality, but the sigmoid fit has clearly defined parameters in terms of energetics, whereas the Arrhenius-type approach leads to a threshold expressed as an effective temperature, which would require yet another conversion to reach an energy scale.

Similar breakdown curves were obtained with all benzylpyridinium ions investigated in that the parent ions $[\text{R-C}_6\text{H}_4\text{-CH}_2\text{-NC}_5\text{H}_5]^+$ disappeared following a sigmoid behavior and resulting in the formation of the $[\text{R-C}_6\text{H}_4\text{-CH}_2]^+$ daughter ions. We note that in several cases other signals resulting from either competing pathways or consecutive reactions of the primary fragments (such as addition of acetonitrile)[45] were observed in small proportions. While the consecutive reactions are summed into the primary dissociation according to Scheme 1, the only competing reactions observed for the compounds under study were a loss of atomic iodine[46,47] for R = *p*-I and of a loss of $\text{NO}_2^{\bullet}$ in the case of the

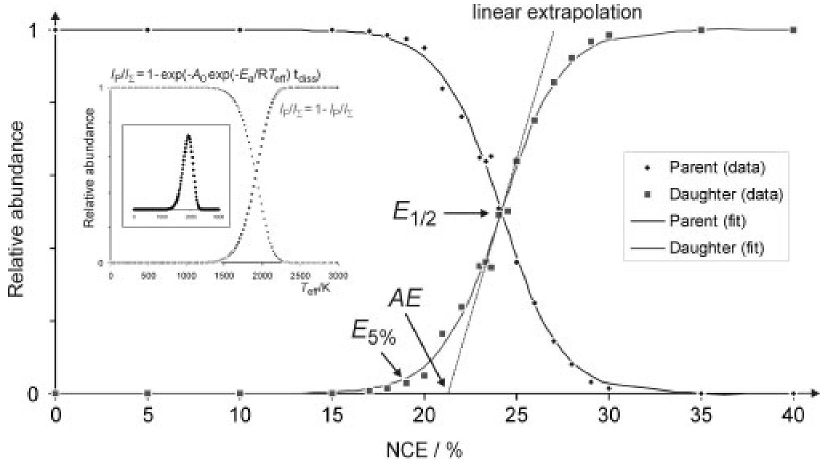

Figure 1. Breakdown diagram of mass-selected $[p\text{-}FC_6H_4\text{-}CH_2\text{-}NC_5H_5]^+$ as a function of the relative collision energy. The dots are the experimental data; the solid lines are the sigmoid functions used for analysis. To assist understanding of the text, the parameters representing the threshold behavior ($E_{5\%}$, AE and $E_{1/2}$) are indicated in the figure. For the description of the inset, see text.

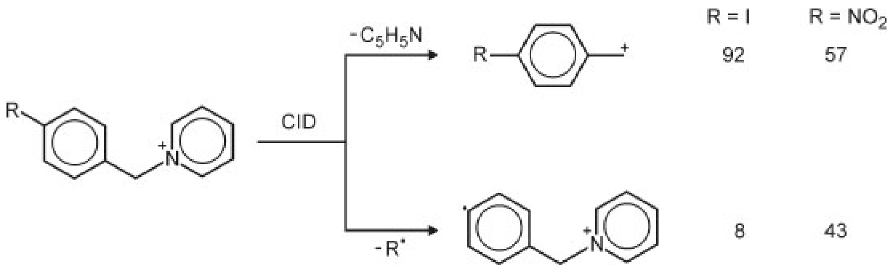

Scheme 2. Radical losses observed upon CID of benzylpyridinium ions with R = I and NO$_2$, respectively. The branching ratios of both channels (normalized to $\Sigma = 100$ for R = I and NO$_2$, respectively) indicated in the scheme correspond to 50% conversion of the parent ions; however, the values were more or less independent of the actual collision energy.

p-NO$_2$ derivative (Scheme 2); due to the pronounced side reaction, the latter compound was excluded from the comparative analysis.

In Table 1, the parameters obtained for modeling the energy-dependent breakdown behaviors of the various benzylpyridinium ions using sigmoid functions are summarized.

The groups of Brodbelt and O'Hair as well as others have extensively used energy-dependent CID in IT-MS before, proposed schemes for the conversion of the apparent thresholds into threshold energies and discussed the most relevant effects, such as excitation time and amplitude, ion mass and ion density of states.[48–62] In the previous approaches for the quantitative analysis of breakdown curves obtained with IT-MS, the energy to bring about a certain amount of fragmentation was considered, e.g. either a small amount (5% or 10%) or 50% parent-ion dissociation,[53,54,60] of which we refer to as $E_{5\%}$ and $E_{50\%}$ in the following; note that for a single fragmentation reaction (i.e. $a_i = 1$), the term $E_{50\%}$ is by definition equal to the parameter $E_{1/2}$ of the sigmoid curves. Here, we suggest the consideration of the respective phenomenological AEs (AE$_{exp}$), i.e. the onset of fragmentation obtained by linear extrapolation of the slope of the breakdown curve at $E_{1/2}$ to the baseline. Compared to $E_{50\%}$, the consideration of AE$_{exp}$ reduces the influence of kinetic effects on the derivation of the underlying intrinsic thermochemistry, where the latter is the property of interest here. Specifically, for a simple bond cleavage (i.e. no barrier in excess of the endothermicity) the rise of the fragment ions from their threshold is *inter alia* determined by the density of states of the parent ion ('size effect'). Larger ions dissociate more slowly such that the resulting

Table 1. Parameters[a,b] obtained in the modeling of the breakdown diagrams of mass-selected pyridinium ions $[R\text{-}C_6H_4\text{-}CH_2\text{-}NC_5H_5]^+$ as a function of the collision energy (in % NCE) with sigmoid functions

Substitution	*B* (% NCE^{-1})	$E_{1/2}$ (% NCE)
H	0.56 ± 0.04	25.75 ± 0.15
o-CH$_3$	0.72 ± 0.05	23.71 ± 0.15
m-CH$_3$	0.65 ± 0.02	24.78 ± 0.05
p-CH$_3$	0.75 ± 0.04	23.15 ± 0.04
2,4-Dimethyl	0.63 ± 0.03	22.16 ± 0.05
2,5-Dimethyl	0.65 ± 0.04	24.04 ± 0.04
3,5-Dimethyl	0.61 ± 0.03	25.13 ± 0.20
p-F	0.67 ± 0.03	24.12 ± 0.05
p-Cl	0.67 ± 0.02	24.56 ± 0.10
p-I	0.71 ± 0.04	23.02 ± 0.05
p-OCH$_3$	0.75 ± 0.02	19.58 ± 0.10
p-CN	0.55 ± 0.05	28.45 ± 0.05
p-CF$_3$	0.58 ± 0.03	28.35 ± 0.10
p-*tert*-Butyl	0.72 ± 0.05[c]	24.29 ± 0.25[c]
Pentamethyl	0.69 ± 0.06	19.88 ± 0.05

[a] C–N bond cleavage according to Scheme 1 was observed almost exclusively; thus, the branching ratio a_i is equal to 1 for all ions studied. Exceptions are R = I and NO$_2$, see Scheme 2.

[b] Error bars estimated from various fits with sigmoid functions that are still in reasonable agreement with the experimental data.

[c] A significantly improved fit is achieved with two sigmoid functions (see text).

Table 2. Selected energetic parameters (given in % NCE) used to describe threshold behaviors derived for the dissociation of benzylpyridinium ions $[\text{R-C}_6\text{H}_4\text{-CH}_2\text{-NC}_5\text{H}_5]^+$ and the calculated appearance energies AE_{calc} (given as $\Delta_r H$ at 0 K in kJ mol^{-1})

Substitution	$E_{5\%}$	$E_{50\%}$	AE_{exp}	AE_{calc}
H	20.4	25.75	22.17	226
o-CH_3	19.5	23.71	20.92	209
m-CH_3	20.3	24.78	21.70	216
p-CH_3	19.0	23.15	20.47	200
2,4-Dimethyl	17.6	22.16	19.00	184
2,5-Dimethyl	19.5	24.19	20.94	198
3,5-Dimethyl	20.3	25.12	21.83	207
p-F	19.9	24.12	21.12	216
p-Cl	19.6	24.56	21.58	213
p-I	18.4	23.05	20.20	198
p-OCH_3	15.6	19.58	16.91	167
p-CN	23.2	28.45	25.05	247
p-CF_3	22.8	28.35	24.89	249
p-*tert*-Butyl	19.5	24.29	21.51	194
Pentamethyl	16.1	19.88	16.98	160

breakdown diagram is flatter, which obviously shifts $E_{1/2}$ to larger values. In the determination of the AE, the extrapolation to the baseline does not eliminate but lowers the effect of the slope on the energetics value derived from $E_{1/2}$.[9,37] Table 2 shows a comparison of the various characteristic values derived from the experimental data obtained for the benzylpyridinium ions investigated with these different approaches.

If we consider the $E_{50\%}$ values, a linear relationship is obtained between the experimental values and the theoretical bond energies (Fig. 2), but the linear regression factor is relatively poor ($R^2 = 0.92$). A similar result is obtained with the $E_{5\%}$ values ($R^2 = 0.93$). The limited correlation coefficients for the linear regressions suggest that the experimental parameters $E_{5\%}$ and $E_{50\%}$ are subject to additional effects other than the mere thresholds, e.g. the densities of states as suggested by Ryzhov and coworkers.[58,60] In comparison, the correlation achieved between the experimental and theoretical AEs is slightly better ($R^2 = 0.96$), and we also prefer this term over $E_{5\%}$ and $E_{50\%}$ because it appears less arbitrary than the choice of a certain percentage of fragmentation. From the linear fit, we receive a conversion factor of 9.8 ± 0.3 kJ mol^{-1} %$^{-1}$ between the % NCE scale and kJ mol^{-1}, where the error is estimated as the standard deviation of all conversion factors derived from the 14 entries in Table 2 (*tert*-butyl not included, see below). This uncertainty is within that of repeated determinations (about ±0.5 in the % NCE scale, see below) and we therefore refrain from a more detailed statistical analysis. We note in passing that the conversion factor of 9.8 ± 0.3 kJ mol^{-1} %$^{-1}$ derived in Fig. 2 agrees with a value of 9.9 ± 0.2 kJ mol^{-1} %$^{-1}$ found in a parallel study of some ionic transition-metal complexes using IT-MS.[9,63] In this context, we point out that deliberately a linear fit that crosses the origin is applied. A reviewer suggested to include an adjustable abscissa, but this does not significantly increase the quality of the fit (e.g. $\text{AE} = 10.6 \times \text{NCE} - 17$ kJ mol^{-1} with $R^2 = 0.964$ vs. $R^2 = 0.959$ for the single-parameter fit $\text{AE} = 9.8 \times \text{NCE}$). Inclusion of a second variable parameter therefore is not indicated. Moreover, as outlined further below the conversion factor is not only instrument dependent but also sensitive to significant changes in the conditions of the IT-MS. In this respect, a single-parameter fit is obviously much more convenient and robust for a rapid re-calibration. We conclude that at least for this family of closely related benzylpyridinium ions, the experimental AEs show a reasonable correlation with the calculated values. However, it is important not to overestimate the approach, because both the assumption of a sigmoid behavior in general and the use of a linear conversion factor in particular are merely phenomenological approaches to ion dissociation, which is fairly more complex.

An often raised criticism against the monitoring of ion/molecule reactions in IT-MS concerns the ill-defined energy distribution of the ions sampled in the trap and this may apply even more so for the various trajectories in CID. Therefore, let us combine the approach using sigmoid fits for energy-resolved multipole experiments[37] with the calibration factor presently derived for IT-MS and turn it around in terms of a determination of the apparent ion internal energy distribution of the benzylpyridinium ions upon CID (Fig. 3). To avoid misunderstanding, we point out that (i) Fig. 3 does not represent the kinetic energy distribution of the incident parent ion but shows the apparent energy content

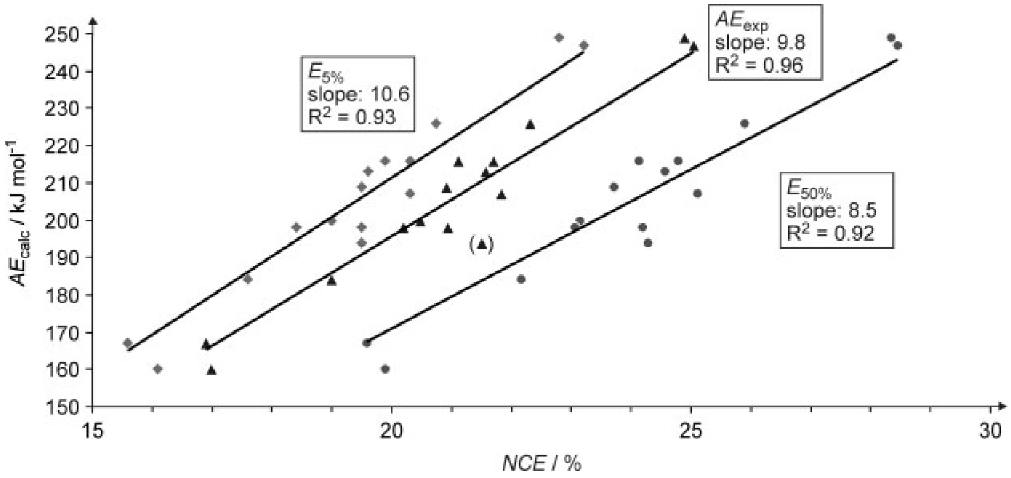

Figure 2. Plot of the characteristic experimental parameters $E_{5\%}$, $E_{50\%}$ and AE_{exp} *versus* the computed values AE_{calc} and the resulting linear equations and correlation coefficients. Note that all correlations are forced to cross the origin. In the correlation of AE *versus* NCE, the point for R = *t*-Bu (triangle in brackets) is not included (see below).

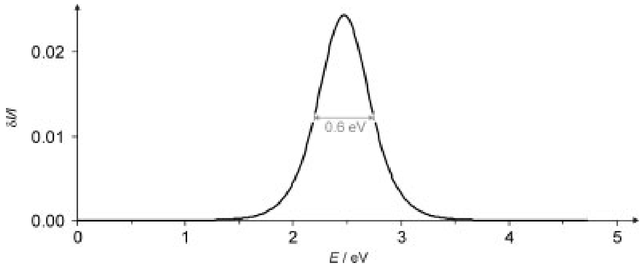

Figure 3. Plot of the derivative of the fitted fragment-ion abundance (data shown in Fig. 1) as a function of the collision energy after conversion to the eV scale.

of the ions upon dissociation and (ii) this treatment neglects the microcanonical dissociation kinetics.[64] Irrespective of these more fundamental reservations, already from the phenomenological half-width in the order of 0.6 eV, even with best data quality we cannot expect a precision better than ±0.1 eV (±10 kJ mol^{-1}) in the resulting AEs. This is a limitation on the one hand, but on the other hand this error margin may pragmatically justify some of the approximations made and also the relatively low number of data points used in the determination of the AEs.

Future work shall test the appropriateness of this simplified analysis, where the effective ion temperature in the trap and simulations of the ion energetics in the trap upon excitation are of particular concern[7]; of the relevant parameters, the excitation time as well as the isolation width appear especially important. In this context we note further that several plots of the values in Table 2 and of the deviations from the correlations in Fig. 2 over other potentially relevant properties (e.g. ion mass, degrees of freedom, absolute AE) scatter randomly and do not reveal any significant correlations, although the ions masses span more than 100 amu (i.e. from *m/z* 170 for R = H to *m/z* 296 for R = *p*-I), the degrees of freedom range from 69 (R = H) to 114 (pentamethyl) and the computed activation energies vary from 160 kJ mol^{-1} (pentamethyl) to 250 kJ mol^{-1} (R = *p*-CF_3). Accordingly, within the experimental uncertainty of the individual measurements we do not see any apparent indications for additional systematic errors in the proposed approach (e.g. due to sizes or masses of the ions), and also no indications for the operation of kinetic shifts are observed. Tentatively, we attribute this fortunate outcome to the multicollisional nature of CID in IT-MS in that ion excitation occurs in a large number of collisions with helium, as a rather light collision gas, resulting in a slow quasi-uniform heating of the parent ions. Combined with the relatively long time of excitation (20 ms), constraints to ion fragmentation due to the dissociation kinetics may thus be bypassed. An admitted limitation is of course the use of computed AE_{calc} as references in the calibration, because the B3P86/6-31+G* method applied is certainly not a 'gold standard' in theoretical chemistry. For example, Barylyuk *et al.*[28] recently conservatively estimated an accuracy of *ca* ±40 kJ mol^{-1} for the critical energies for the dissociation of benzylpyridinium ions predicted with B3LYP/6-311+G(2d,p)//B3LYP/6-31G(d). Nevertheless, an extensive calibration of various DFT and wave-function-based methods with different basis sets has identified the B3P86/6-31+G* approach used here as the best compromise between accuracy and computational costs for the specific case of benzylpyridinium ions.[65] Moreover, many conceivable errors are likely to cancel in the consideration of such a limited set of closely related compounds. Hence, even if an improved level of theory might affect the calibration factor, the correlation between the experimental and theoretical AEs itself is likely to hold.

As mentioned above, the entry for R = *t*-butyl was left out in the correlation shown in Fig. 2. In fact, the breakdown behavior of this particular ion cannot well be described by a sigmoid fit because either the smooth early onset is not reproduced or the relatively steep approach to unity cannot be modeled. While the energy-dependent CID in IT-MS may have its pitfalls in the method itself, for the other ions the sigmoid approximation works reasonably well (Fig. 1, for example). Moreover, there is a chemical reason for the deviating behavior in the case of R = *t*-butyl. Specifically, we have previously shown by means of consecutive reactions with neutral toluene[66] that CID of this particular pyridinium ion leads to a *ca* 70 : 30 mixture of the *tert*-butyl benzylium ion as the product of direct bond cleavage and the *tert*-butyl tropylium ion formed via rearrangement (Scheme 3).[32]

An improved fit of the experimental data can be achieved, if two sigmoid functions are used (Fig. 4), of which we attribute the first to the structural rearrangement leading to the tropylium isomer, whereas the second sigmoid is assigned to the direct C-N bond cleavage to afford the benzylium ion. Consistent with this view, the first sigmoid has lower values of $E_{1/2}$ and *b* than the second, i.e. $E_{1/2}$ = 21.6% NCE and *b* = 0.77 versus $E_{1/2}$ = 25.1% NCE and *b* = 1.11. Note that for a rearrangement reaction one would expect even a decreasing yield at elevated energies,[38,39] which cannot be described by a simple sigmoid curve. As both reactions lead to fragment ions of the same *m/z* ratio, there is no point in considering such an additional channel, however, because only the sum of both isomers is the experimental variable. For the same reason, we refrain from a further analysis of the convoluted sigmoid curves in terms of AEs.

In a more general perspective, the conversion factor derived above is instrument specific and accordingly should be re-determined, whenever instrumentation and/or fundamental parameters are changed. In order to illustrate the transferability of the proposed method to a different IT-MS of the same supplier, Fig. 5 shows three CID experiments for R = H obtained with two different IT-MS using identical activation parameters.

Table 3 allows to compare the corresponding parameters *b*, $E_{1/2}$ and AE obtained from sigmoid fits of these experimental data. Specifically, each series of measurements was used to perform three different fits: one with the smallest and one with the largest value of *b* which still fits the data and the best fit with an average value of *b*; $E_{1/2}$ was then optimized accordingly for each value of *b*, because changes in *b* can in part be compensated by variation of $E_{1/2}$. From the range of acceptable fit parameters, the standard deviations of the parameters were obtained.

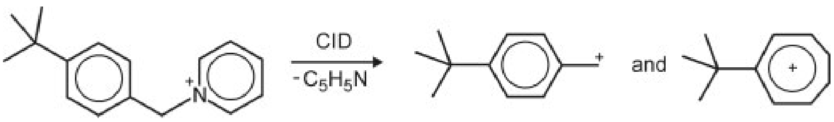

Scheme 3. Formation of isomeric product ions upon CID of benzylpyridinium ions with R = *t*-Bu.

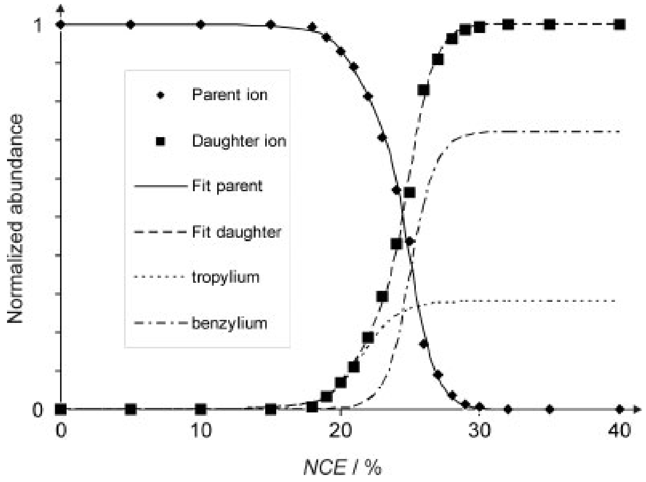

Figure 4. Breakdown diagram of mass-selected [t-Bu-C_6H_4-CH_2-NC_5H_5]$^+$ as a function of the relative collision energy. The dots are the experimental data; the solid lines are the sigmoid functions used for analysis.

Table 3. Comparison of the experimental parameters obtained from three series of CID experiments (data shown in Fig. 3) in the case of the fragmentation of the non-substituted benzylpyridinium ion (R = H)

	LCQ, Prague	LCQ, Prague[a]	Deca XP, Paris
b (% NCE^{-1})	0.54 ± 0.03	0.57 ± 0.03	0.56 ± 0.04
$E_{1/2}$ (% NCE)	26.25 ± 0.18	26.05 ± 0.17	25.75 ± 0.15
AE (% NCE)	22.40 ± 0.32	22.45 ± 0.24	22.17 ± 0.28

[a] Independent repetition on a different day.

While some spread of the data is obvious, the reasonably close agreement achieved between the CID parameters obtained on two different mass spectrometers further indicates the applicability of the approach presented here for the estimation of the CID threshold energies of the benzylpyridinium ions under study.

As a warning we add, however, that an independent repetition of the experiments with R = t-butyl on the Deca XP more than a year after the original data set has been recorded and with an extended period of repair and maintenance led to a significant shift of the $E_{1/2}$ value by about 1% NCE. Similarly, the associated AE derived from the data was shifted, whereas the shapes of the breakdown curves were superimposable within the experimental error. The exact origin of this perturbation could not be elucidated after the maintenance, but it appears most likely that the helium pressure in the trap changed, because in the LCQ this is directly adjusted by the backing pressure of helium. Similarly, a re-calibration of the LCQ in Prague after a significant modification of the helium inlet of the trap for a set of five benzylpyridinium ions showed a good linear correlation, but a shift of the scaling factor of 9.8 ± 0.3 kJ mol^{-1} %$^{-1}$ derived from Fig. 2 to 8.4 ± 0.3 kJ mol^{-1} %$^{-1}$ after the modification. These findings re-iterate the obvious fact that any calibration needs to be checked in regular intervals and after any manipulation of the instrument hardware, which is another reason why we prefer a single-parameter calibration which can be performed rather rapidly.

Conclusions

From studies of a series of benzylpyridinium ions frequently used as thermometer molecules, a simple scheme for the conversion of nominal collision energies in an IT-MS into an absolute energy scale is proposed. To this end, the phenomenological AEs derived from the CID breakdown curves of the benzylpyridinium ions are correlated with calculated reaction endothermicities. The reasonably good correlation achieved is promising with regard to the use of IT-MS for the simple and rapid estimation of reaction energies in the gas phase. The validity of the concept will form a subject of forthcoming studies, and we explicitly invite other groups to engage in this testing, because IT-MS is a particularly widespread and also rather simple technique with versatile applications.[6,7] Already now it is obvious, however, that the conversion scheme is an empirical calibration which has to be controlled in regular intervals and renewed whenever the parameters of the ion trap are modified (helium pressure,

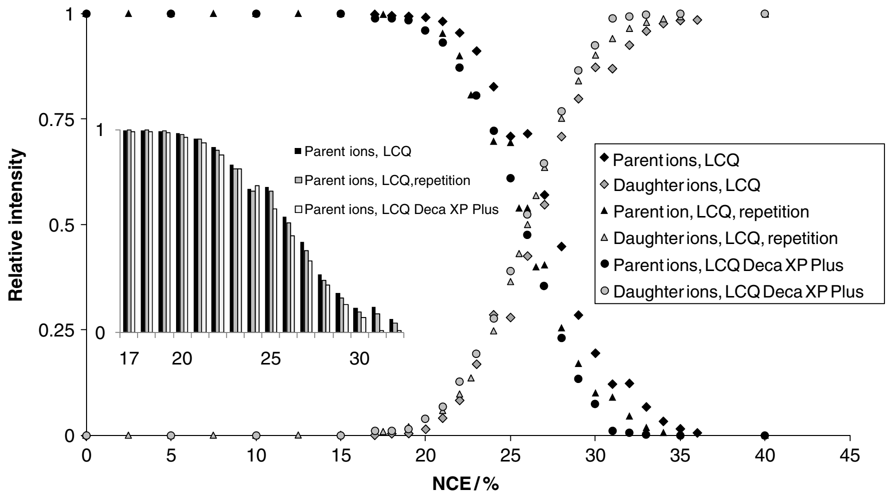

Figure 5. Breakdown diagrams of mass-selected [C_6H_5-CH_2-NC_5H_5]$^+$ as a function of relative collision energies obtained on two different ion-trap mass spectrometers using the same excitation parameters. The inset shows the same set of data (only for the parent ion) and aids in the direct comparison of the separate series of experiments.

excitation time, isolation width, etc.). Otherwise, at least for the benzylium ions as a set of closely related compounds, neither mass effects nor an influence of the density of states is observed with the procedure proposed. Tentatively, we ascribe this result to the multicollisional nature of CID in IT-MS and the consideration of extrapolated AEs that are less sensitive to the dissociation kinetics of the parent ions than reference to a certain amount of parent-ion fragmentation. In the specific case of the (*p-tert*-butylbenzyl)pyridinium ion, the energy-dependent CID spectra further suggest the formation of the rearranged tropylium isomer upon low-energy CID, whereas the direct C-N bond cleavage to afford the corresponding benzylium ion prevails at higher energies. This conclusion derived from the energy-dependent CID experiments is consistent with earlier findings based on ion/molecule reactions of the fragments formed from the (*p-tert*-butylbenzyl)pyridinium ion.[32]

Acknowledgements

This work was supported by the Academy of Sciences of the Czech Republic (Z40550506) and the European Research Council (AdG HORIZOMS). We thank K. Barylyuk and R. Zenobi for additional details about the calculations reported in Ref. [28].

References

[1] R. G. Cooks, P. S. H. Wong. Kinetic method of making thermochemical determinations: advances and applications. *Acc. Chem. Res.* **1998**, *31*, 379.
[2] W. Shen, P. S. H. Wong, R. G. Cooks. Stereoisomeric distinction by the kinetic method: 2,3-butanediol. *Rapid Commun. Mass Spectrom.* **1997**, *11*, 71.
[3] P. B. Armentrout. Kinetic energy dependence of ion-molecule reactions: guided ion beams and threshold measurements. *Int. J. Mass Spectrom.* **2000**, *200*, 219.
[4] K. M. Ervin. Experimental techniques in gas-phase ion thermochemistry. *Chem. Rev.* **2001**, *101*, 391.
[5] P. B. Armentrout, K. M. Ervin, M. T. Rodgers. Statistical rate theory and kinetic energy-resolved ion chemistry: theory and applications. *J. Phys. Chem. A* **2008**, *112*, 10071.
[6] R. A. J. O'Hair. The 3D quadrupole ion trap mass spectrometer as a complete chemical laboratory for fundamental gas-phase studies of metal mediated chemistry. *Chem. Commun.* **2006**, 1469.
[7] S. Gronert. Quadrupole ion trap studies of fundamental organic reactions. *Mass Spectrom. Rev.* **2005**, *24*, 100.
[8] Normalized collision energy™ technology. Finnigan Product Support Bull. 104. http://www.thermo.com/eThermo/CMA/PDFs/Articles/articlesFile_21418.pdf.
[9] Á. Révész, P. Milko, J. Žabka, D. Schröder, J. Roithová. Reduction from copper(II) to copper(I) upon collisional activation of (pyridine)$_2$CuCl$^+$. *J. Mass Spectrom* (in press). DOI: 10.1002/jms.1793.
[10] F. Derwa, E. de Pauw, P. Natalis. New basis for a method for the estimation of secondary ion internal energy distribution in "soft" ionization techniques. *Org. Mass Spectrom.* **1991**, *26*, 117.
[11] C. Collette, E. de Pauw. Calibration of the internal energy distribution of ions produced by electrospray. *Rapid Commun. Mass Spectrom.* **1998**, *12*, 165.
[12] G. H. Luo, I. Marginean, A. Vertes. Internal energy of ions generated by matrix-assisted laser desorption/ionization. *Anal. Chem.* **2002**, *74*, 6185.
[13] J. F. Greisch, V. Gabelica, F. Remacle, E. de Pauw. Thermometer ions for matrix-enhanced laser desorption/ionization internal energy calibration. *Rapid Commun. Mass Spectrom.* **2003**, *17*, 1847.
[14] V. Gabelica, E. Schulz, M. Karas. Internal energy build-up in matrix-assisted laser desorption/ionization. *J. Mass Spectrom.* **2004**, *39*, 579.
[15] J. Naban-Maillet, D. Lesage, A. Bossee, Y. Gimbert, J. Sztaray, K. Vekey, J. C. Tabet. Internal energy distribution in electrospray ionization. *J. Mass Spectrom.* **2005**, *40*, 1.
[16] V. Gabelica, E. de Pauw. Internal energy and fragmentation of ions produced in electrospray sources. *Mass Spectrom. Rev.* **2005**, *24*, 566.
[17] G. H. Luo, Y. Chen, G. Siuzdak, A. Vertes. Surface modification and laser pulse length effects on internal energy transfer in DIOS. *J. Phys. Chem. B* **2005**, *109*, 24450.
[18] S. L. Luxembourg, R. M. A. Heeren. Fragmentation at and above surfaces in SIMS: effects of biomolecular yield enhancing surface modifications. *Int. J. Mass Spectrom.* **2006**, *253*, 181.
[19] E. Schulz, M. Karas, F. Rosu, V. Gabelica. Influence of the matrix on analyte fragmentation in atmospheric pressure MALDI. *J. Am. Soc. Mass Spectrom.* **2006**, *17*, 1005.
[20] G. H. Luo, Y. Chen, H. Daniels, R. Dubrow, A. Vertes. Internal energy transfer in laser desorption/ionization from silicon nanowires. *J. Phys. Chem. B* **2006**, *110*, 13381.
[21] D. Touboul, M. C. Jecklin, R. Zenobi. Ion internal energy distributions validate the charge residue model for small molecule ion formation by spray methods. *Rapid Commun. Mass Spectrom.* **2008**, *22*, 1062.
[22] A. Pak, D. Lesage, Y. Gimbert, K. Vekey, J. C. Tabet. Internal energy distribution of peptides in electrospray ionization: ESI and collision-induced dissociation spectra calculation. *J. Mass Spectrom.* **2008**, *43*, 447.
[23] M. Nefliu, J. N. Smith, A. Venter, R. G. Cooks. Internal energy distributions in desorption electrospray ionization (DESI). *J. Am. Soc. Mass Spectrom.* **2008**, *19*, 420.
[24] Y. S. Xiao, S. T. Retterer, D. K. Thomas, J. Y. Tao, L. He. Impacts of surface morphology on ion desorption on porous silicon (DIOS) mass spectrometry. *J. Phys. Chem. C* **2009**, *113*, 3076.
[25] P. Lecchi, J. H. Zhao, W. S. Wiggins, T. H. Chen, P. F. Yip, B. S. Mansfield, J. M. Peltier. A method for monitoring and controlling reproducibility of intensity data in complex electrospray mass spectra: a thermometer ion-based strategy. *J. Am. Soc. Mass Spectrom.* **2009**, *20*, 398.
[26] H. W. Tang, K. M. Ng, W. Lu, C. M. Che. Ion desorption efficiency and internal energy transfer in carbon-based surface-assisted laser desorption/ionization mass spectrometry: desorption mechanism(s) and the design of SALDI substrates. *Anal. Chem.* **2009**, *81*, 4720.
[27] S. Dagan, Y. M. Hua, D. J. Boday, A. Somogyi, R. J. Wysocki, V. H. Wysocki. Internal energy deposition with silicon nanoparticle-assisted laser desorption/ionization (SPALDI) mass spectrometry. *Int. J. Mass Spectrom.* **2009**, *283*, 200.
[28] K. V. Barylyuk, K. Chingin, R. M. Balabin, R. Zenobi. Fragmentation of benzylpyridinium "thermometer" ions and its effect on the accuracy of internal energy calibration. *J. Am. Soc. Mass Spectrom.* **2010**, *21*, 172.
[29] G. A. Harris, D. M. Hostetler, C. Y. Hampton, F. M. Fernandez. Comparison of the internal energy deposition of direct analysis in real time and electrospray ionization time-of-flight mass spectrometry. *J. Am. Soc. Mass Spectrom.* **2010**, *21*, 855.
[30] E. L. Zins, C. Pepe, D. Rondeau, S. Rochut, N. Galland, J. C. Tabet. Theoretical and experimental study of tropylium formation from substituted benzylpyridinium species. *J. Mass Spectrom.* **2009**, *44*, 12.
[31] E. L. Zins, D. Rondeau, P. Karoyan, C. Fosse, S. Rochut, C. Pepe. Investigations of the fragmentation pathways of benzylpyridinium ions under ESI/MS conditions. *J. Mass Spectrom.* **2009**, *44*, 1668.
[32] E. L. Zins, C. Pepe, D. Schröder. Selectivites and internal-energy effects in the methylene-transfer reactions of substituted benzylium/tropylium ions with neutral toluene. *Faraday Discuss.* **2010**, *145*, 157.
[33] A. Hoxha, C. Collette, E. de Pauw, B. Ley. Mechanism of collisional heating in electrospray mass spectrometry: ion trajectory calculations. *J. Phys. Chem. A* **2001**, *105*, 7326.
[34] A. Tintaru, J. Roithová, D. Schröder, L. Charles, I. Jušinski, Z. Glasovac, M. Eckert-Maksić. Generation and dissociation pathways of singly and doubly protonated bisguanidines in the gas phase. *J. Phys. Chem. A* **2008**, *112*, 12097.
[35] N. B. Cech, C. G. Enke. Practical implications of some recent studies in electrospray ionization fundamentals. *Mass Spectrom. Rev.* **2001**, *20*, 362.
[36] D. Schröder, T. Weiske, H. Schwarz. Dissociation behavior of Cu(urea)$^+$ complexes generated by electrospray ionization. *Int. J. Mass Spectrom.* **2002**, *219*, 729.

[37] D. Schröder, M. Engeser, M. Brönstrup, C. Daniel, J. Spandl, H. Hartl. Ion chemistry of the hexanuclear methoxo-oxovanadium cluster $V_6O_7(OCH_3)_{12}$. *Int. J. Mass Spectrom.* **2003**, *228*, 743.

[38] C. Trage, M. Diefenbach, D. Schröder, H. Schwarz. Innocent and less-innocent solvent ligands: a systematic investigation of cationic iron/alcohol complexes by electrospray ionization mass spectrometry complemented by DFT calculations. *Chemistry* **2006**, *12*, 2454.

[39] P. Gruene, C. Trage, D. Schröder, H. Schwarz. Solvent- and ligand effects on the structure of iron-halide cations in the gas phase. *Eur. J. Inorg. Chem.* **2006**, 4546.

[40] D. Schröder, M. Engeser, H. Schwarz, E. C. E. Rosenthal, J. Döbler, J. Sauer. Degradation of ionized $OV(OCH_3)_3$ in the gas phase. From the neutral compound all the way down to the quasi-terminal fragments VOH^+ and VO^+. *Inorg. Chem.* **2006**, *45*, 6235.

[41] G. Bouchoux, D. Leblanc, J. Y. Salpin. A relationship between the kinetics and thermochemistry of proton transfer reactions in the gas phase. *Int. J. Mass Spectrom.* **1996**, *153*, 37.

[42] Gaussian, Inc. *Gaussian 03, Revision E.01*, Gaussian, Inc.: Wallingford, CT, **2004**.

[43] T. Fujiwara, E. C. Lim. Binding energies of the neutral and ionic clusters of naphthalene in their ground electronic states. *J. Phys. Chem. A* **2003**, *107*, 4381.

[44] R. B. Metz, C. Nicolas, M. Ahmed, S. R. Leone. Direct determination of the ionization energy of FeO and CuO with VUV radiation. *J. Chem. Phys.* **2005**, *123*, 114313.

[45] V. Gabelica, D. Lemaire, O. Laprevote, E. de Pauw. Kinetics of solvent addition on electropsrayed ions in an electrospray source and in a quadrupole ion trap. *Int. J. Mass Spectrom.* **2001**, *210*, 113.

[46] L. J. Chyall, H. I. Kentämaa. The 4-dehydroanilinium ion – a stable distonic isomer of ionized aniline. *J. Am. Chem. Soc.* **1994**, *116*, 3135.

[47] K. K. Thoen, R. L. Smith, J. J. Nousiainen, E. D. Nelson, H. I. Kentämaa. Charged phenyl radicals. *J. Am. Chem. Soc.* **1996**, *118*, 8669.

[48] A. Colorado, J. Brodbelt. An empirical approach to estimation of critical energies by using a quadrupole ion trap. *J. Am. Soc. Mass Spectrom.* **1996**, *7*, 1116.

[49] M. Satterfield, J. S. Brodbelt. Relative binding energies of gas-phase pyridyl ligand/metal complexes by energy-variable collisionally activated dissociation in a quadrupole ion trap. *Inorg. Chem.* **2001**, *40*, 5393.

[50] M. L. Reyzer, J. S. Brodbelt, S. M. Kerwin, D. Kumar. Evaluation of complexation of metal-mediated DNA-binding drugs to oligonucleotides via electrospray ionization mass spectrometry. *Nucleic Acid Res.* **2001**, *29*, E103.

[51] W. M. David, J. S. Brodbelt. Threshold dissociation energies of protonated amine/polyether complexes in a quadrupole ion trap. *J. Am. Soc. Mass Spectrom.* **2003**, *14*, 383.

[52] M. C. Crowe, J. S. Brodbelt. Evaluation of noncovalent interactions between peptides and polyether compounds via energy-variable collisionally activated dissociation. *J. Am. Soc. Mass Spectrom.* **2003**, *14*, 1148.

[53] J. M. Zhang, J. S. Brodbelt. Threshold dissociation and molecular modelling of transition metal complexes of flavonoids. *J. Am. Soc. Mass Spectrom.* **2005**, *16*, 139.

[54] T. Waters, R. A. J. O'Hair, A. G. Wedd. Catalytic gas phase oxidation of methanol to formaldehyde. *J. Am. Chem. Soc.* **2003**, *125*, 3384.

[55] R. A. J. O'Hair, A. K. Vrkic, P. F. James. Gas-phase synthesis and reactivity of the organomagnesates $[CH_3MgL_2]^-$ (L = Cl and O_2CCH_3): from ligand effects to catalysis. *J. Am. Chem. Soc.* **2004**, *126*, 12173.

[56] G. N. Khairallah, R. A. J. O'Hair. Gas-phase synthesis of $[Ag_4H]^+$ and its mediation of the C–C coupling of allyl bromide. *Angew. Chem. Int. Ed.* **2005**, *44*, 728.

[57] K. J. Hart, S. A. McLuckey. Relative dissociation-energy measurements using ion-trap collisional activation. *J. Am. Soc. Mass Spectrom.* **1994**, *5*, 250.

[58] E. E. Jellen, A. M. Chappell, V. Ryzhov. Effects of size of noncovalent complexes on their stability during collision-induced dissociation. *Rapid Commun. Mass Spectrom.* **2002**, *16*, 1799.

[59] L. A. Hayes, A. M. Chappell, E. E. Jellen, V. Ryzhov. Binding of metalloporphyrins to model nitrogen bases: collision-induced dissociation and ion-molecule reaction studies. *Int. J. Mass Spectrom.* **2003**, *227*, 111.

[60] N. Vinokur, V. Ryzhov. Using collision-induced dissociation with corrections for the ion number of degrees of freedom for quick comparisons of relative bonding strength. *J. Mass Spectrom.* **2004**, *39*, 1268.

[61] T. Gozet, L. Huynh, D. K. Bohme. Collision-induced dissociation of tetraphenyl iron and manganese porphyrin ions by electrospray ionization mass spectrometry. *Int. J. Mass Spectrom.* **2009**, *279*, 113.

[62] A. M. Fernandes, J. A. P. Coutinho, I. M. Marrucho. Gas-phase dissociation of ionic liquid aggregates studied by electrospray ionisation mass spectrometry and energy-variable collision induced dissociation. *J. Mass Spectrom.* **2009**, *44*, 144.

[63] D. Schröder, L. Ducháčková, I. Jušinski, M. Eckert-Maksić, J. Heyda, L. Tůma, P. Jungwirth. Characterization of the triple ion $[(CH_3)_4N^+PF_6^-\,(CH_3)_4N^+]$ in the gas phase. *Chem. Phys. Lett.* **2010**, *490*, 14.

[64] D. Rondeau, N. Galland, E. Zins, C. Pepe, L. Drahos, K. Vékey. Internal energy distribution of ions observed in an electrospray source interfaced with a sector mass spectrometer. *J. Mass Spectrom.* (submitted for publication).

[65] E. L. Zins. Etude theoretique et experimentale par ESI/MS/MS de complexes cationises de bases nucleiques, et de la fragmentation d'ions benzylpyridinium. PhD Thesis, Université Pierre et Marie Curie, Paris, **2009**.

[66] T. D. Fridgen, J. Troe, A. A. Viggiano, A. J. Midey, S. Williams, T. B. McMahon. Experimental and theoretical studies of the benzylium$^+$/tropylium$^+$ ratios after charge exchange to ethylbenzene. *J. Phys. Chem. A* **2004**, *108*, 5600.